in vivo *27*: 233-244 (2013)

Changes of Metabolic Profiles in an Oral Squamous Cell Carcinoma Cell Line Induced by Eugenol

TEHO KOH[1], YUKIO MURAKAMI[1], SHOJI TANAKA[1], MAMORU MACHINO[1], HIROMI ONUMA[3], MIKU KANEKO[3], MASAHIRO SUGIMOTO[3,4], TOMOYOSHI SOGA[3], MASARU TOMITA[3] and HIROSHI SAKAGAMI[2]

Divisions of [1]Oral Diagnosis and [2]Pharmacology, Meikai University School of Dentistry, Sakado, Saitama, Japan; [3]Institute for Advanced Biosciences, Keio University, Tsuruoka, Yamagata, Japan; [4]Graduate School of Medicine and Faculty of Medicine, Kyoto University, Sakyo-ku, Kyoto, Japan

Abstract. *Background: We have recently reported that eugenol exerted indiscriminate cytotoxicity towards normal oral cells and oral squamous cell carcinoma (OSCC) cell lines without induction of apoptosis markers. In order to investigate the underlying mechanisms of cytotoxicity induction, we investigated the effect of short-term treatment with eugenol on the metabolic profiles of a human OSCC cell line (HSC-2). Materials and Methods: The viable cell number was determined by direct cell counting with a hemocytometer after trypsinization. After washing with 5% D-mannitol solution (found to retain the highest amounts of intracellular metabolites among several washing conditions), cellular metabolites were extracted with methanol with internal markers and then subjected to metabolomic analysis. Results: Cytotoxic concentrations of eugenol induced the reduction of ATP utilization (assessed by a significant reduction of the AMP/ATP and ADP/ATP ratio), of oxidative stress (assessed by the increase in oxidized form of glutathione, cysteine-glutathione disulfide and methionine sulfoxide), and an increase in the polyamines and glycolytic metabolites. Conclusion: The metabolic changes observed in this study suggest the induction of non-apoptotic cell death by eugenol.*

Zinc oxide-eugenol formulations have been used in dentistry for many years as bases, liners, cements and temporary restorative materials (1), and in a survey conducted in 1997, zinc-oxide-eugenol was cited as the preferred material for root canal fillings (2). On the other hand, it is known that zinc oxide-eugenol releases eugenol in concentrations that are cytotoxic (3), and one human clinical study showed that zinc oxide-eugenol induced chronic inflammation, no pulp healing and no dentin bridge formation up to 12 weeks postoperatively, as compared to healing with capping with calcium hydroxide (4). However, due to the small number of samples, the lack of randomized clinical trials and of long-term follow-up studies, and the absence of proper coronal sealing, whether eugenol is the best root canal filling material for endodontically-treated deciduous teeth, is still questionable (5, 6).

Induction of cytotoxicity by eugenol has been reported to be very rapid and irreversible (7, 8), and eugenol damaged both human normal oral cells (gingival fibroblast, pulp cells and periodontal ligament fibroblasts) and oral squamous cell carcinoma cell lines (HSC-2, HSC-4, Ca9-22), to comparable extents, as assessed from similar 50% cytotoxic concentrations (CC_{50}) for both normal and tumor cells (8). Eugenol has been reported to induce different types of cell death; apoptosis in human promyelocytic leukemia (9), colon cancer (10) and breast cancer cells (11), and non-apoptosis in human normal oral cells and oral squamous cell carcinoma cell lines (8).

Apoptosis and necrosis are two alternative forms of cell death, with well-defined morphological and biochemical differences (12). One crucial physiological difference between cells that undergo apoptosis and these undergoing necrosis is the intracellular ATP levels. Since apoptosis is an energy-dependent process, a decrease in ATP to below critical levels may impede the execution of apoptosis and promote necrosis (13, 14). In order to analyze the eugenol-induced cell death in greater detail, we investigated the effect of eugenol on the concentrations of various cellular metabolites including ATP in the human oral squamous cell

Correspondence to: Professor Hiroshi Sakagami, Division of Pharmacology, Meikai University School of Dentistry, Sakado, Saitama 350-0283, Japan. Tel: +81 492792758, Fax: +81 492855171, e-mail: sakagami@dent.meikai.ac.jp

Key Words: Eugenol, non-apoptotic cell death, oral squamous cell carcinoma, metabolomics, ATP utilization, oxidative stress, polyamine, HSC-2 cells.

carcinoma cell line HSC-2. We have reported that the 50% cytotoxicity concentrations (CC_{50}) of eugenol against HSC-2 cells was 0.7 mM, and 4 h was the minimum incubation time required for the induction of irreversible non-apoptotic cell death, characterized by the lack of induction of internucleosomal DNA fragmentation and caspase-3 activation (8). In the present study, we used the following conditions: eugenol concentration of 0.7, 1.4 and 2.8 mM, and an incubation time of 4 h.

Materials and Methods

Materials. The following chemicals and materials were obtained from the indicated companies: Dulbecco's modified Eagle's medium (DMEM) from Gibco BRL, Grand Island, NY, USA; fetal bovine serum (FBS), eugenol (MW=164), dimethylsulfoxide (DMSO) from Wako Pure Chemical, Osaka, Japan; 10-cm dish from Becton Dickinson Labware, Franklin Lakes, NJ, USA. Eugenol was dissolved in DMSO at 200 mM before use, and diluted with medium. Treatment of HSC-2 cells with 0 or 1.4% DMSO-alone resulted in only a 2.6% decrease of the viable cell number after 4 h incubation ($5.29\pm0.47\times10^6$ cells (0% DMSO), *vs*. $5.15\pm0.94\times10^6$ cells (1.4% DMSO).

Eugenol treatment. The human oral squamous cell carcinoma cell line HSC-2 was kindly provided by Professor Nagumo, Showa University, Japan, and was cultured in DMEM supplemented with 10% heat-inactivated FBS. HSC-2 cells (3×10^5) were inoculated on a 10-cm dish (Becton Dickinson Labware) and grown to near confluency. After replacing medium with fresh culture medium, cells were treated for 4 h without (control) or with 0.7 mM (corresponding to the CC_{50}), 1.4 mM ($2\times CC_{50}$) or 2.8 mM ($4\times CC_{50}$) of eugenol in quadruplicate. The cell numbers recovered from one 10-cm dish after treatment for 4 h with 0, 0.7 1.4 and 2.8 mM eugenol were 2.80, 2.65, 2.43 and 1.85×10^6 cells on the average, respectively. The cells were washed twice with 5 ml of ice-cold 5% D-mannitol and then immersed for 10 min with 1 ml methanol containing internal standard (25 μmol/l each of methionine sulfone, 2-[*N*-morpholino]-ethanesulfonic acid and D-camphor-10-sulfonic acid). The methanol extract (supernatant) was collected and frozen at –80˚C until capillary electrophoresis time-of-flight mass spectrometry (CE-TOF-MS) analysis, as described below. The relative viable cell number was determined by direct cell counting with hemocytometer after trypsinization.

Sample preparation for CE-TOF-MS. In 400 μl of the dissolved samples, 400 μl of chloroform and 200 μl of Milli-Q water were added and the mixture was centrifuged at 10,000 ×*g*, for 3 min at 4˚C. The aqueous layer was filtered to remove large molecules by centrifugation through a 5-kDa cut-off filter (Millipore, Billerica, MA, USA) at 9,100 ×*g* for 3 h at 4˚C. The filtrate (320 μl) was concentrated by centrifugation and dissolved in 50 μl of Milli-Q water containing reference compounds (200 μmol/l each of 3-aminopyrrolidine and trimesate), immediately before CE-TOF-MS analysis.

CE-TOF-MS analysis. The instrumentation and measurement conditions used for CE-TOF-MS are described elsewhere (15-18) with slight modifications. Briefly, cation analysis was performed using an Agilent CE capillary electrophoresis system, an Agilent G6220A LC/MSD-TOF system, an Agilent 1100 series isocratic HPLC pump, a G1603A Agilent CE-MS adapter kit, and a G1607A Agilent CE-electrospray ionization (ESI)-MS sprayer kit (Agilent Technologies, Waldbronn, Germany). Anion analysis was performed using an Agilent CE capillary electrophoresis system, an Agilent G6210A LC/MSD TOF system, an Agilent 1200 series isocratic HPLC pump, a G1603A Agilent CE-MS adapter kit, and a G1607A Agilent CE-ESI source-MS sprayer kit (Agilent Technologies). For the cation and anion analyses, the CE-MS adapter kit includes a capillary cassette that facilitates thermostatic control of the capillary. The CE-ESI-MS sprayer kit simplifies coupling of the CE system with the MS system, and is equipped with an electrospray source. For system control and data acquisition, we used the G2201AA Agilent ChemStation software for CE and the Agilent MassHunter software for TOF-MS. The original Agilent SST316Ti stainless steel ESI needle was replaced with a passivated SST316Ti stainless steel and platinum needle (passivated with 1% formic acid and 20% aqueous solution of isopropanol at 80˚C for 30 min) for anion analysis (16).

For cationic metabolite analysis using CE-TOF-MS, sample separation was performed in fused silica capillaries (50 μmi.d. ×100 cm total length) filled with 1 M formic acid as the reference electrolyte. The capillary was flushed with formic acid (1 M) for 20 min before the first use and for 4 min before each sample injection. Sample solutions (3 nl) were injected at 50 mbar for 5 s and a voltage of 30 kV was applied. The capillary temperature was maintained at 20˚C and the temperature of the sample tray was kept below 5˚C. The sheath liquid, composed of methanol/water (50% v/v) and 0.1 μmol/lhexakis (2,2-difluoroethoxy) phosphazene (Hexakis), was delivered at 10 μl/min. ESI-TOF-MS was conducted in the positive ion mode. The capillary voltage was set at 4 kV and the flow rate of nitrogen gas (heater temperature=300˚C)

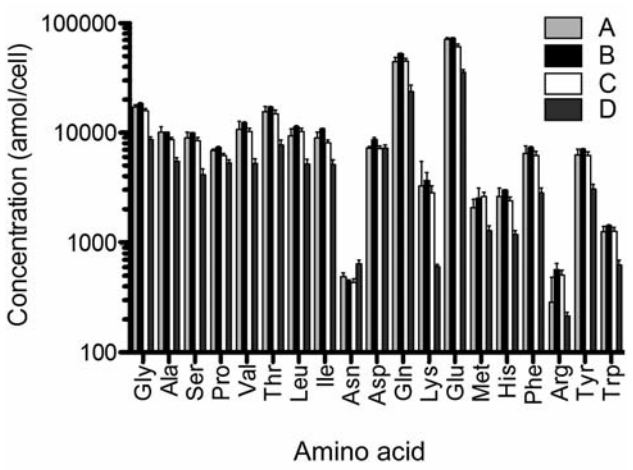

Figure 1. *Loss of amino acids during the cell washing procedure. HSC-2 cells (2.3×10^6/10-cm dish) were washed twice with either 5% D-mannitol (37˚C) (A), 5% D-mannitol (0˚C) (B), phosphate-buffered saline without calcium and magnesium [PBS (–)](C), or PBS(–) after cell harvesting with 0.25%] trypsinization (D), and then intracellular metabolites were extracted with methanol. Intracellular amino acid concentration was plotted without and with (not shown) correction for loss by multiplying the area ratio of the internal standard (IS). Each value is the mean of quadruplicate samples±standard deviation (S.D.).*

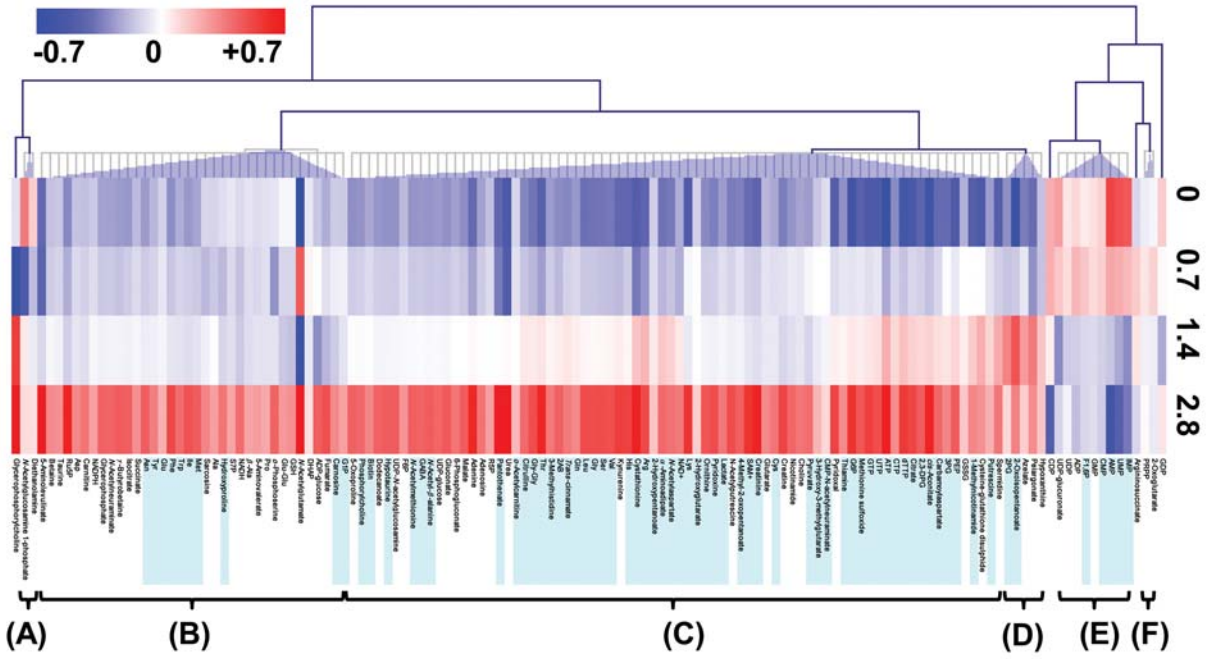

Figure 2. *Heat map and bar graph visualization of the quantified metabolites. Heat map showing the quantified matabolites using a blue–white-red scheme. Red and blue indicates that the averaged inter-cellular metabolites were relatively higher and lower, respectively, for each metabolite. The labels (A) to (F) are the representative metabolite clusters. The values of 0, 0.7, 1.4 and 2.8 indicate the concentration (mM) of eugenol used. Concentrations of the metabolites colored in light blue were significantly different (q-value <0.05) in the cells treated with 1.4 mM of eugenol, compared to the untreated (control) cells.*

was set at 7 psig. In TOF-MS, the fragmentor, skimmer and OCT RF voltages were 75, 50 and 125 V, respectively. Automatic re-calibration of each acquired spectrum was performed using reference standards {[^{13}C isotopic ion of protonated methanol dimer (2MeOH + H)]$^+$, *m/z* 66.0632)} and {[protonated Hexakis (M + H)]$^+$, *m/z* 622.0290]}. Mass spectra were acquired at the rate of 1.5 cycles/s over an m/z range of 50-1,000.

For anionic metabolite analysis using CE-TOF-MS, a commercially-available COSMO(+) capillary (50 μmi.d. ×105 cm, NacalaiTesque, Kyoto, Japan), chemically-coated with a cationic polymer, was used for separation. Ammonium acetate solution (50 mmol/l; pH 8.5) was used as the electrolyte for separation. Before the first use, the new capillary was flushed successively with the running electrolyte (pH 8.5), 50 mmol/l acetic acid (pH 3.4), and then the electrolyte again for 10 min each. Before each injection, the capillary was equilibrated for 2 min by flushing with 50 mM acetic acid (pH 3.4) and was then flushed for 5 min with the running electrolyte. A sample solution (30 nl) was injected at 50 mbar for 30 s, and a voltage of –30 kV was applied. The capillary temperature was maintained at 20˚C and the sample tray was cooled below 5˚C. An Agilent 1100 series pump equipped with a 1:100 splitter was used to deliver 10 μl/min of 5 mM ammonium acetate in 50% (v/v) methanol/water, containing 0.1 μM Hexakis, to the CE interface. Here, it was used as a sheath liquid surrounding the CE capillary to provide a stable electrical connection between the tip of the capillary and the grounded electrospray needle. ESI-TOF-MS was conducted in the negative ionization mode at a capillary voltage of 3.5 kV. For TOF-MS, the fragmentor, skimmer and OCT RF voltages were set at 100, 50 and 200 V, respectively. The flow rate of the drying nitrogen gas (heater temperature=300˚C) was maintained at 7 psig. Automatic re-calibration of each acquired spectrum was performed using reference standards {[[^{13}C isotopic ion of deprotonated acetic acid dimer (2 CH_3COOH-H)]$^-$, *m/z* 120.03841} and {[Hexakis+deprotonated acetic acid (M+CH_3COOH-H)]$^-$, an *m/z* 680.03554}. Exact mass data were acquired at a rate of 1.5 spectra/s over an *m/z* range of 50-1,000. We have searched a total of 578 compounds (310 cationic and 268 anionic) including various metabolic pathways.

Data processing. Raw data were analyzed by our proprietary software MasterHands (18), which follows typical data processing flows including detecting all possible peaks, eliminating noise and redundant features, and generating the aligned data matrix with annotated metabolite identities and relative area (peak areas normalized by those of internal standards) (19). Concentrations were calculated using external standards based on relative area.

Preparation of heat map. The amount of each metabolite was expressed as the molar concentration per single cell (amol/cell). Only metabolites that were detectable in more than 60% of 16 samples (n≥10) were used. The concentration of each metabolite was averaged among quadruplicate samples, converted by a factor of log 2 (to increase the contrast of color intensity), and then subtracted by the mean values calculated in all groups per each metabolite to determine the color for the heat map. The mean value is expressed by a white color. The Pearson's correlation was used for clustering metabolites.

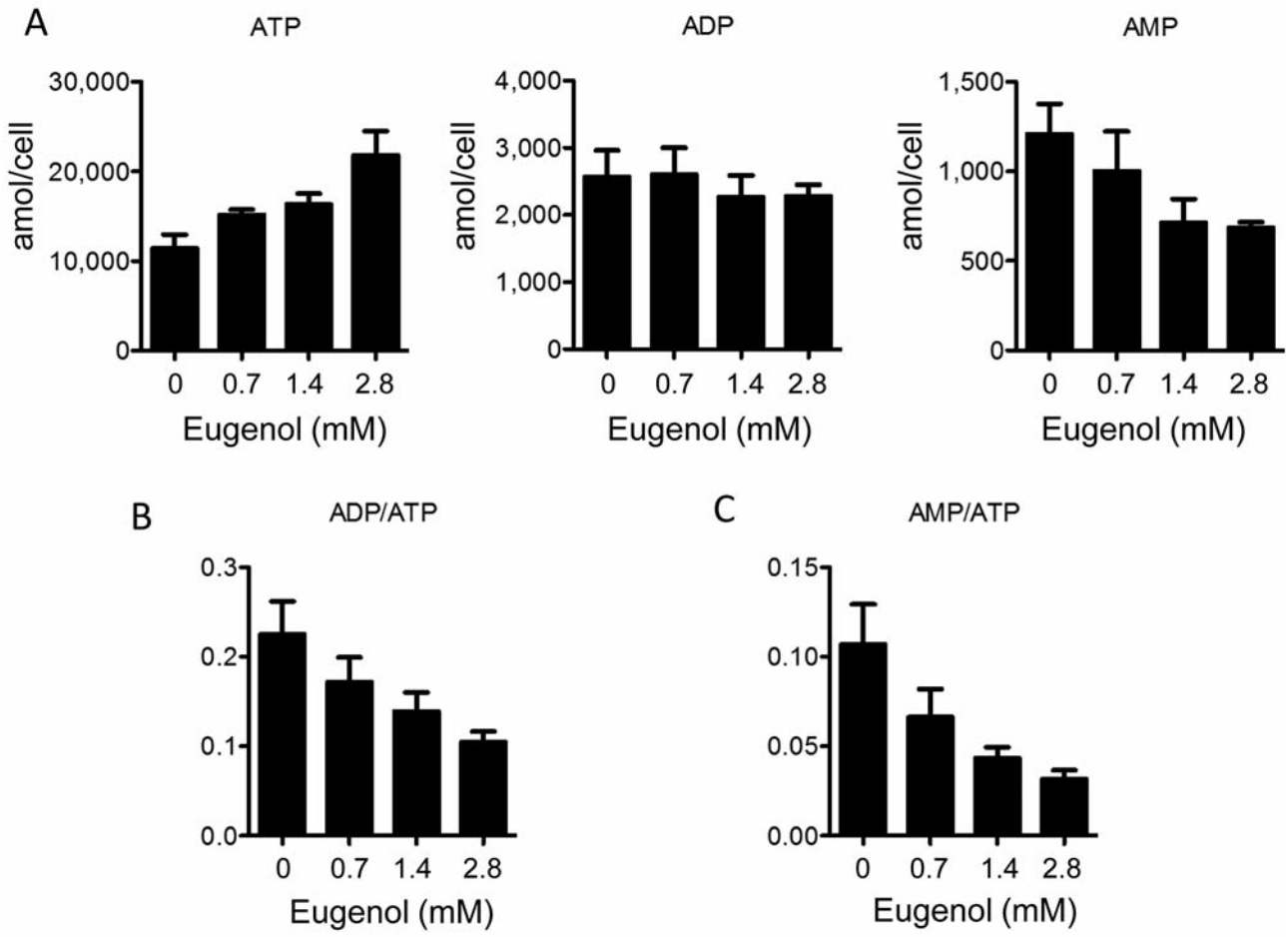

Figure 3. *Changes in the intracellular concentrations of ATP, ADP and AMP (A), and ADP/ATP ratio (B), AMP/ATP ratio (C) after treatment for 4 h with the indicated concentrations of eugenol. Each value is the mean of quadruplicate samples ±S.D.*

Statistical analysis. Student's *t*-test (two-tailed) was used for statistical comparison between the metabolite concentrations in the cells treated without (control) and these treated with 1.4 mM of eugenol. To account for multiple testing, we calculated *q*-values, a false discovery rate (FDA), for all *p*-values (20), and a *q*-value <0.05 was considered as statistically significant. Data analyses and visualization were conducted using R-software (2.14.0) and Mev TM4 software (version 4.7.4. Dana-Farber Cancer Institute, Boston, MA, USA) (21).

Results

Selection of best washing solution for metabolomics analysis. It was important to minimize the leak of intracellular metabolites during the washing process. Therefore, we first selected the washing buffer that retained the greatest amounts of all metabolites (Figure 1). Washing with 5% D-mannitol solution, whether pre-warmed (37˚C) (A) or chilled (0˚C) (B), resulted in a higher recovery of all amino acids, as compared with washing with phosphate-buffered saline without calcium and magnesium (PBS(–))(C). Cell harvest by 0.25% trypsin-0.025% EDTA in PBS(–), resulted in a significant loss of intracellular amino acids (D). Similar trends were observed after the correction by internal standard (IS). Washing with pre-warmed 5% D-mannitol solution, but not with chilled 5% D-mannitol solution, resulted in the slight decrease of arginine. Based on these data, chilled 5% D-mannitol solution was used for cell washing in the subsequent experiments.

Overview of the detected metabolites. A total of 150 substances were identified and, out of these, 134 were used for clustering analysis (Figure 2). Overall, metabolites were separated into six clusters (labeled A to F). The intracellular concentrations of most of the metabolites increased with an increase in eugenol concentration (clusters B to D). Cluster D metabolites exhibited a higher increase in the intracellular concentration at 1.4 mM eugenol, as compared with cluster B and C. Meanwhile, metabolites in clusters F, and especially

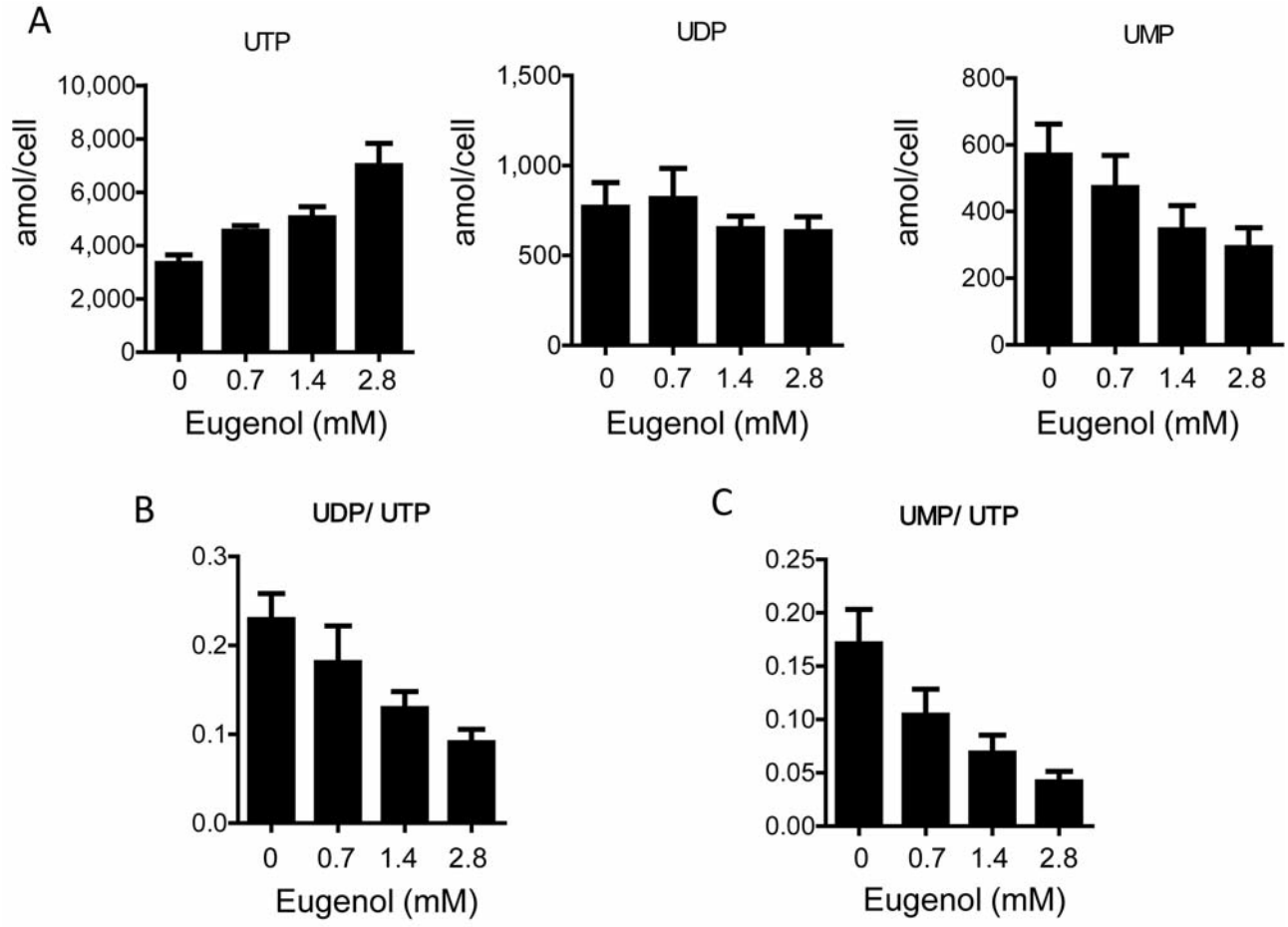

Figure 4. *Changes in the intracellular concentrations of UTP, UDP and UMP (A), and the UDP/UTP (B) and UMP/UTP (C) ratios after treatment for 4 h with the indicated concentrations of eugenol. Each value is the mean of quadruplicate samples ±S.D.*

cluster E, exhibited a decreasing tendency for intracellular concentration with an increase in eugenol concentration.

Among cluster E metabolites, compounds that are involved in ATP metabolism markedly declined. All amino acids with an increase in eugenol concentration were included in clusters B and C. Other clusters included a variety of types of metabolites. We compared data at 0 and 1.4 mM eugenol, since a higher concentration (2.8 mM) devastatingly damaged the cells, causing rather non-specific alterations in many metabolites.

Decline of ATP utilization. With an increase in eugenol concentrations, the ATP concentration increased (Figure 3A). On the other hand, the ADP concentration was slightly reduced (Figure 3A), resulting in a 53% decline of the ADP/ATP ratio (Figure 3B). Similarly, the AMP concentration markedly declined (Figure 3A), resulting in a 70% decline of the AMP/ATP ratio (Figure 3C). This indicates the significant reduction of ATP utilization into ADP and AMP.

With an increase in eugenol concentration, the UTP concentration was increased. On the other hand, the UDP concentration was reduced (Figure 4A), resulting in a 60% decline of UDP/UTP ratio (Figure 4B). Similarly, the UMP concentration declined (Figure 4A), resulting in 75% decline of the UMP/UTP ratio (Figure 4C).

The GTP concentration was increased with an increase in eugenol concentrations (Figure 5A). Since GDP and GMP concentrations did not change significantly (Figure 5A), the GDP/GTP and GMP/GTP ratios declined (Figure 5B, C), but to relatively low extents (49 and 55%, respectively).

Changes in glycolytic pathway and tricarboxylic acid (TCA) cycle. Eugenol treatment induced slight elevation of the intracellular concentrations of the metabolites involved in the glycolytic pathway: 3-phospho-D-glyceric acid (Figure 6A), 2-phospho-D-glyceric acid (Figure 6B), phosphoenol pyruvate (Figure 6C) and an end product of glycolysis pathway, lactate. On the other hand, changes in the

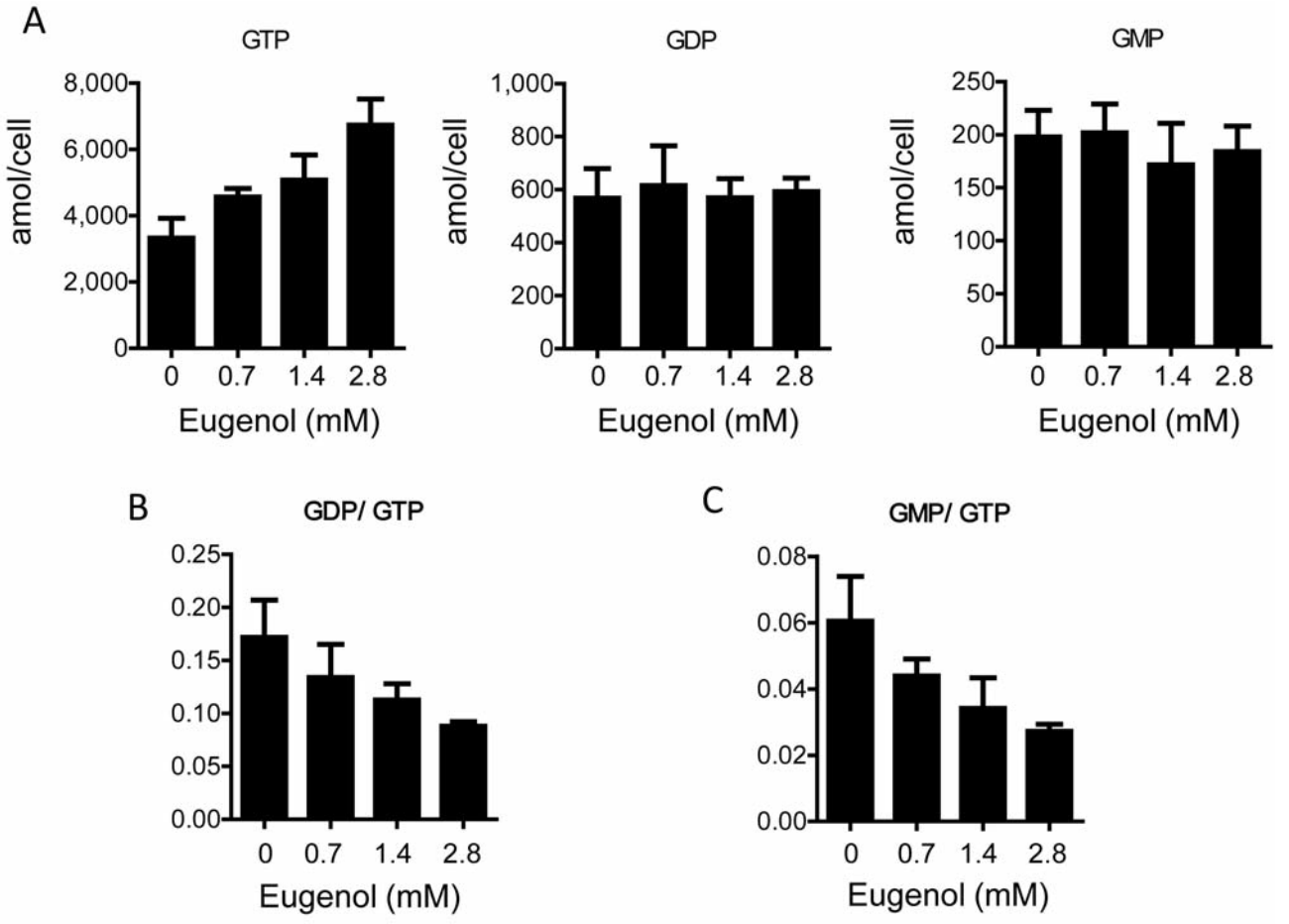

Figure 5. *Changes in the intracellular concentrations of GTP, GDP and GMP (A), and the GDP/GTP (B) and GMP/GTP (C) ratios after treatment for 4 h with the indicated concentrations of eugenol. Each value is the mean of quadruplicate samples ±S.D.*

metabolites of the TCA cycle were relatively small: succinate (Figure 6D), isocitrate (Figure 6E), fumarate (Figure 6F) and 2-oxoglutarate (Figure 6G).

Changes in redox compounds. Eugenol treatment more potently increased the intracellular concentration of the oxidized form of glutathione, as compared with the reduced form of glutathione, thus increasing the ratio of the oxidized form/reduced form by 69% at maximum (Figure 7A). The intracellular concentrations of cysteine (Figure 7B), cystathionine and cysteine-glutathione disulphide (Figure 7C) were also increased. It should be noted that the increase of cysteine-glutathione disulfide, a molecule that is formed upon oxidative stress of gluthathione, reached 203% that of the control at the maximum (Figure 7C). All these data clearly show that eugenol induced oxidative stress in HSC-2 cells.

Methionine is known to be oxidized into methionine sulfoxide. Eugenol treatment increased the intracellular concentration of methionine sulfoxide (Figure 8A) more potently than that of methionine (Figure 8B), resulting in an increase in the ratio of methionine sulfoxide/methione by 37% (Figure 8C), further supporting the induction of oxidative stress by eugenol.

Changes in polyamines. Eugenol treatment stimulated polyamine synthesis, as judged by the increase in the intracellular concentration of putrescine (Figure 9A) spermidine (Figure 9B) and ornithine (Figure 9C).

Changes in amino acids. Eugenol treatment slightly increased the total intracellular concentration of amino acids (Figure 10A), but did not affect the ratio of glycine to total amino acids (Figure 10B). Eugenol changed the intracellular concentration of proline to a lesser extent, since the ratio of proline to total amino acids rather declined slightly with an increase in eugenol concentration (Figure 10C).

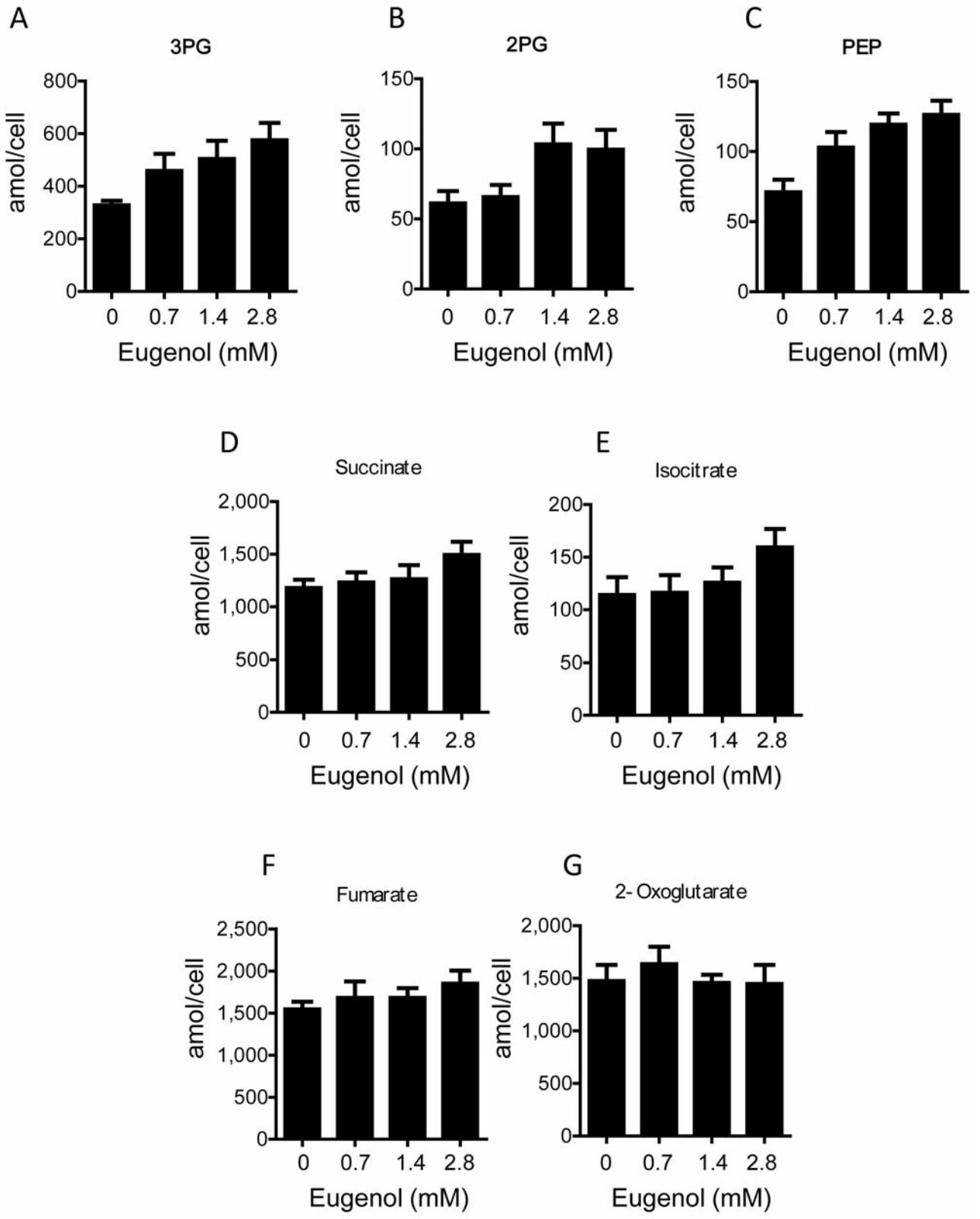

Figure 6. *Changes in the intracellular concentrations of 3-phospho-D-glyceric acid (3PG) (A), 2-phospho-D-glyceric acid (2PG) (B), phosphoenol pyruvate (PEP) (C), succinate (D), isocitrate (E), fumarate (F) and 2-oxoglutarate (G) after treatment for 4 h with the indicated concentrations of eugenol. Each value is the mean of quadruplicate samples ±S.D.*

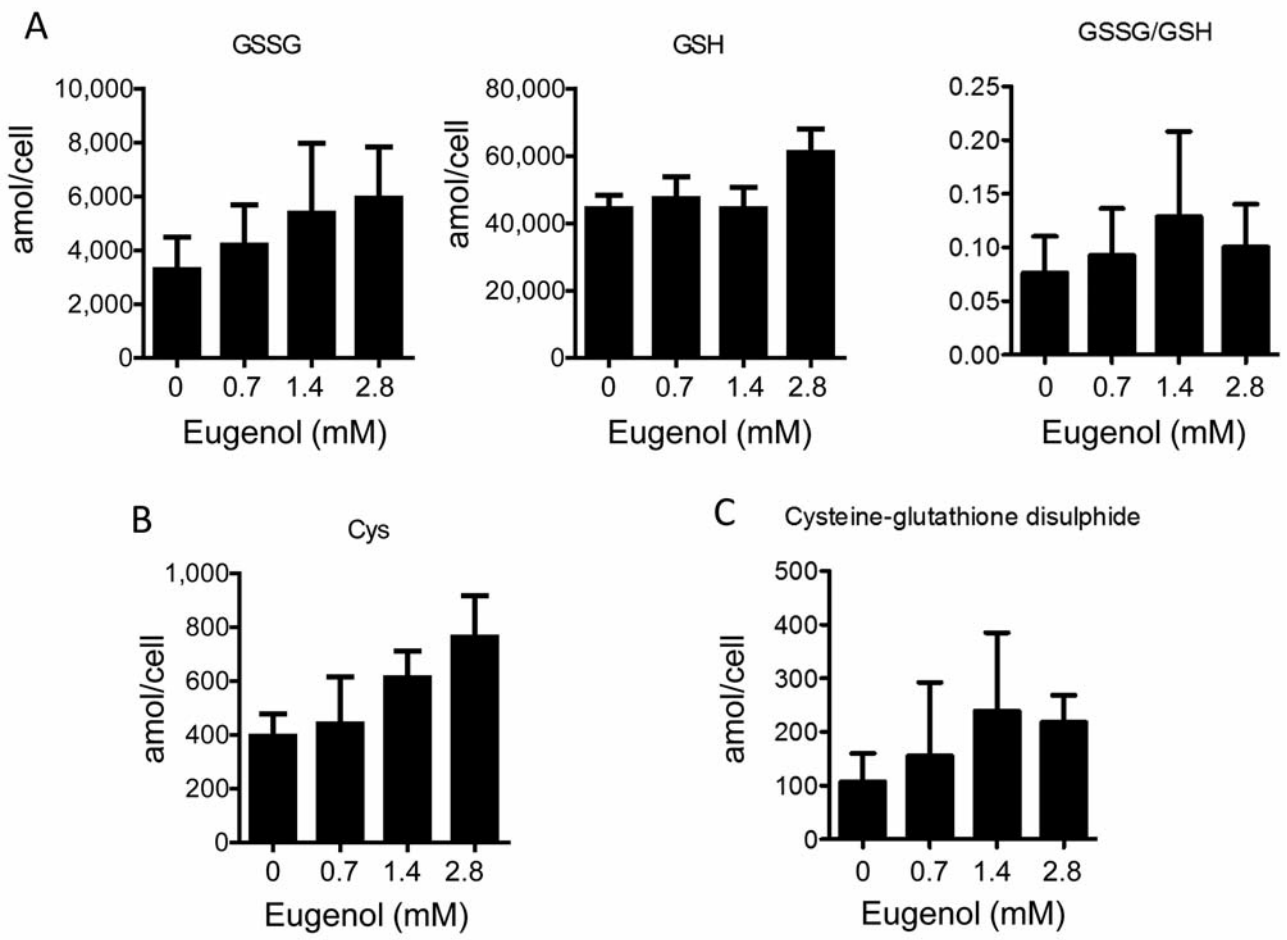

Figure 7. *Changes in the intracellular concentration of oxidized form of glutathione (GSSG), reduced form of glutathione (GSH) and ratio of GSSG/GSH (A). Changes in the intracellular concentration of cysteine (B), cysteine-glutathione disulphide (C) after treatment for 4 h with the indicated concentrations of eugenol. Each value is the mean of quadruplicate samples ±S.D.*

Discussion

The present study demonstrated that eugenol reduced the ATP utilization, but increased the polyamine levels in the cells. The reduction of ATP utilization may disturb many cellular processes that require ATP, and direct the cells toward necrotic cell death rather than apoptosis. The increase of polyamine levels may reflect the emergent response of cells to repair membrane damage (possibly induced by lipid layer breaks), since polyamines influence actin re-organization and motility, and thus modify the membranes function (22, 23).

It has been reported that the addition of *N*-acetyl-L-cysteine, but not superoxide dismutase and catalase, protected human osteoblastic cells from eugenol-induced cytotoxicity, suggesting that the inhibitory effects were associated with the level of gluthatione (24). Eugenol has been also reported to reduce the intracellular levels of gluthathione and increase the lipid peroxidation products (thiobarbituric acid reactive substances) in breast cancer cell lines (11). The present study supports and extends the results of these reports, by first providing evidence that eugenol induced the accumulation of cysteine-glutathione disulfide, a molecule formed upon oxidative stress of gluthathione (25). Furthermore, we demonstrated that eugenol increased the intracellular accumulation of methionine sulfoxide, an oxidation product of methionine (26). All these data strongly suggest that eugenol induced oxidative stress in HSC-2 cells.

Among these factors, only oxidative stress markers [(i) of oxidized form of glutathione/reduced form of glutathione, (ii) cysteine-glutathione disulphide, (iii) ratio of methionine sulfoxide/methionine] and polyamines (spermine and spermidine) reached a maximum at 1.4 mM eugenol, whereas other markers (ATP, ADP/ATP, AMP/ATP, UTP, UDP/UTP, UMP/UTP, glycolytic pathway metabolites, TCA

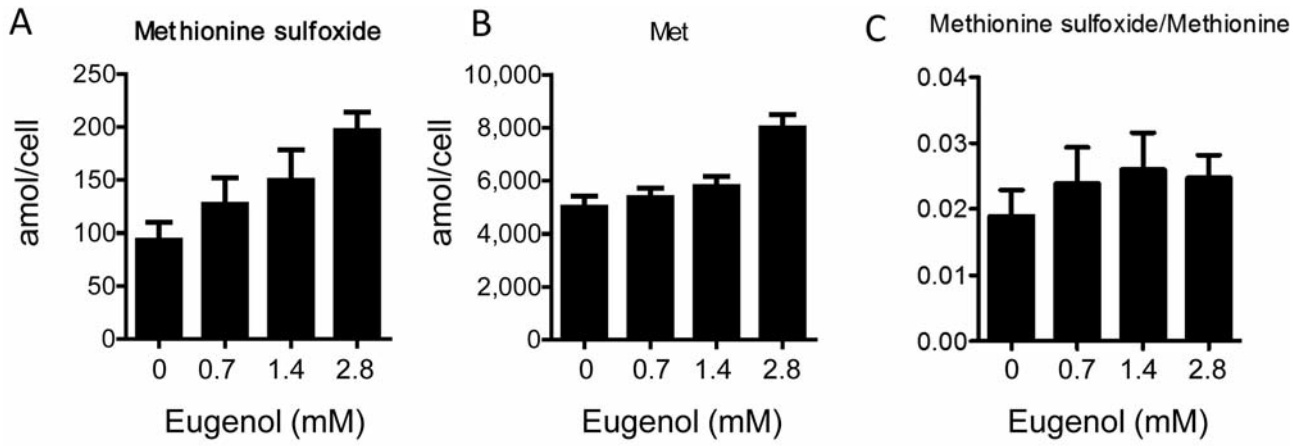

Figure 8. *Changes in the intracellular concentrations of methionine sulfoxide (A) and methionine (B), and the ratio of methionine sulfoxide/methionine (C) after treatment for 4 h with the indicated concentrations of eugenol. Each value is the mean of quadruplicate samples ±S.D.*

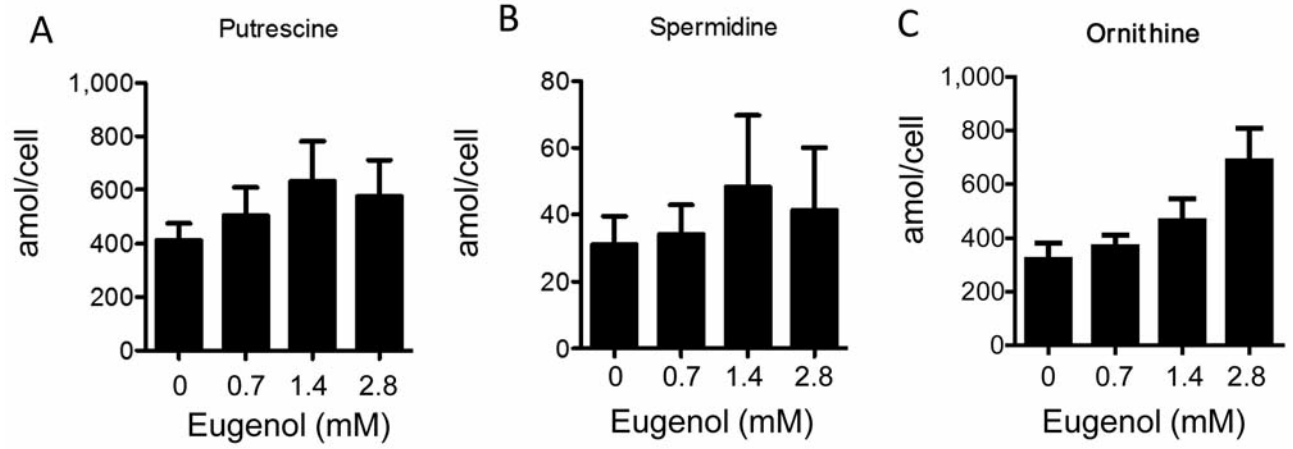

Figure 9. *Changes in the intracellular concentrations of putrescine (A), spermidine (B) and ornithine (C) after treatment for 4 h with the indicated concentrations of eugenol. Each value is the mean of quadruplicate samples ±S.D.*

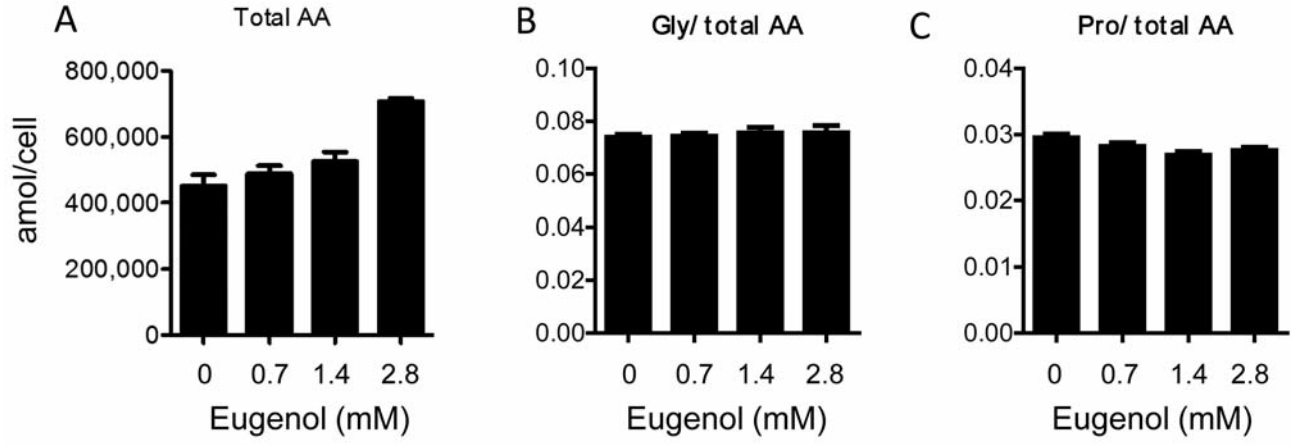

Figure 10. *Changes in the intracellular concentrations of total amino acids (AA) (A), ratio of glycine to total AA (B) and the ratio of proline to total AA (C) after treatment for 4 h with the indicated concentrations of eugenol. Each value is the mean of quadruplicate samples ±S.D.*

cycle metabolites) increased up to 2.8 mM eugenol. Based on these facts, we propose the after sequence of intracellular events after eugenol treatment. Eugenol firstly induces oxidative stress, secondly membrane damage and repair (polyamine synthesis required), and finally decline of ATP utilization. A detailed time-course study is needed to confirm this hypothesis.

We recently found that eugenol significantly enhanced interleukin (IL)-8 production by IL-1β-stimulated human gingival fibroblasts, whereas it stimulated or inhibited IL-8 production by human pulp cells at lower and higher concentrations, respectively (27). This points to the possibility that eugenol further aggravates inflammation accompanied by induction of necrosis. This pro-inflammatory action of eugenol on human gingival fibroblasts is quite different from the lipopolysaccharide-activated mouse macrophage system where eugenol had an anti-inflammatory action (28, 29), as well as its direct superoxide-scavenging action (30, 31). The different results between gingival fibroblasts and macrophages may be due to the different cytokine production systems.

Considering the very narrow safety margin, careful oral treatment with eugenol is necessary. Although eugenol is non-genotoxic to human pulp cell cultures (32), care should be taken to reduce the possibility of pulpal as well as periapical irritations from inadvertent extrusion in clinical usage.

Finally, we investigated the possible changes in glycine and proline after treatment with eugenol, since we have recently found that among salivary amino acids, glycine and proline exhibited unique changes during aging (33) and in the recovery process after template therapy (34). The present study demonstrated that intracellular concentrations of both glycine and proline had similar patterns of increase to those of other amino acids, suggesting that these amino acids are not specific targets of eugenol-induced cell death.

References

1 Sweet C: Procedure for treatment of expoxed and pulpless deciduous teeth. J Am Dent Assoc *17*: 1150-1153, 1930.

2 Primosch RE: Primary tooth pulp therapy as taught in predoctoral pediatric dental programs in the United States. Pediatr Dent *19*: 118-122, 1997.

3 Hume W: An analysis of the release and the diffusion through dentin of eugenol from zinc oxide-eugenol mixtures. J Dent Res *63*: 881-884, 1984.

4 Glass R and Zander H: Pulp healing. J Dent Res *28*: 97-107, 1949.

5 Barja-Fidalgo F, Moutinho-Ribeiro M, Oliveira MAA and Oliveira BH: A systemic review of root canal filling materials for deciduous teeth: Is there an alternative for zinc oxide-eugenol? ISRN Dentistry Volume 2011, Article ID367318, 7 pages doi:10.5402/2011/367318.

6 Hilton TJ: Keys to clinical success with pulp capping: A review of the literature. Oper Dent *34*: 615-625, 2009.

7 Hume WR: Effect of eugenol on respiration and division in human pulp, mouse fibroblasts, and liver cells *in vitro*. J Dent Res *63*: 1262-1265, 1984.

8 Koh T, Machino M, Murakami Y, Umemura N and Sakagami H: Cytotoxicity of dental compounds against human oral squamous cell carcinoma and normal oral cells. In Vivo *27*: 85-96, 2013.

9 Atsumi T, Fujisawa S, Satoh K, Sakagami H, Iwakura I, Ueha T, Sugita Y and Yokoe I: Cytotoxicity and radical intensity of eugenol, isoeugenol or related dimers. Anticancer Res *20*: 2519-2524, 2000.

10 Jaqanathan SK, Mazumdar A, Mondhe D and Mandal M: Apoptotic effect of eugenol in human colon cancer cell lines. Cell Biol Int *35*: 607-615, 2011.

11 Vidhya N and Devaraj SN: Induction of apoptosis by eugenol in human breast cancer cells. Indian J Exp Biol *49*: 871-878, 2011.

12 Majno G and Joris I: Apoptosis, oncosis, and necrosis. An overview of cell death. Am J Pathol *146*: 3-15, 1995

13 Halestrap AP, Clarke SJ and Javadov SA: Mitochondrial permeability transition pore opening during myocardial reperfusion – a target for cardioprotection. Cardiovasc Res *61*: 372-385, 2004.

14 Halestrap A: Biochemistry: a pore way to die. Nature *434*: 578-579, 2005.

15 Soga T, Baran R, Suematsu M, Ueno Y, Ikeda S, Sakurakawa T, Kakazu Y, Ishikawa T, Robert M, Nishioka T and Tomita M: Differential metabolomics reveals ophthalmic acid as an oxidative stress biomarker indicating hepatic glutathione consumption. J Biol Chem *281*: 16768-16776, 2006.

16 Soga T, Igarashi K, Ito C, Mizobuchi K, Zimmermann HP and Tomita M: Metabolomic profiling of anionic metabolites by capillary electrophoresis mass spectrometry. Anal Chem *81*: 6165-6174, 2009.

17 Sugimoto M, Sakagami H, Yokote Y, Onuma H, Kaneko M, Mori M, Sakaguchi Y, Soga T and Tomita M: Non-targeted metabolite profiling in activated macrophage secretion. Metabolomics *8*: 624-633, 2012.

18 Sugimoto M, Wong DT, Hirayama A, Soga T and Tomita M: Capillary electrophoresis mass spectrometry-based saliva metabolomics identified oral, breast and pancreatic cancer-specific profiles. Metabolomics *6*: 78-95, 2010.

19 Sugimoto M, Kawakami M, Robert M, Soga T and Tomita M: Bioinformatics tools for mass spectroscopy-based metabolomic data processing and analysis. Curr Bioinform *7*: 96-108, 2012.

20 Storey JD and Tibshirani R: Statistical significance for genomewide studies. Proc Natl Acad Sci USA *100*: 9440-9445, 2003.

21 Saeed AI, Sharov V, White J, Li J, Liang W, Bhagabati N, Braisted J, Klapa M, Currier T, Thiagarajan M, Sturn A, Snuffin M, Rezantsev A, Popov D, Ryltsov A, Kostukovich E, Borisovsky I, Liu Z, Vinsavich A, Trush V and Quackenbush J: TM4: A free, open-source system for microarray data management and analysis. Biotechniques *34*: 374-378, 2003.

22 Cobum RF: Polyamine effects on cell function: Possible central role of plasma membrane PI(4,5)P2. J Cell Physiol *221*: 544-551, 2009.

23 Xie LH, John SA, Ribalet B and Weiss JN: Activation of inwardly rectifying potassium (Kir) channels by phosphatidylinositol-4,5-bisphosphate (PIP2): interaction with other regulatory ligands. Prog Biophys Mol Biol *94*: 320-335, 2006.

24 Ho YC, Huang FM and Chang YC: Mechanisms of cytotoxicity of eugenol in human osteoblastic cells *in vitro*. Int Endod J *39*: 389-393, 2006.
25 Yoshiba-Suzuki S, Sagara J, Bannai S and Makino N: The dynamics of cysteine, glutathione and their disulphides in astrocyte culture medium. J Biochem *150*: 95-102, 2011.
26 Tarrago L and Gladyshev VN: Recharging oxidative protein repair: catalysis by methionine sulfoxide reductases towards their amino acid, protein, and model substrates. Biochemistry *77*: 1097-1107, 2012.
27 Koh T, Murakami Y, Tanaka S, Machino M and Sakagami H: Re-evaluation of anti-inflammatory potential of eugenol in IL-1B-stimulated gingival fibroblast and pulp cells. In Vivo *27*: in press, 2013.
28 Magalhães CB, Riva DR, DePaula LJ, Brando-Lima A, Koatz VL, Leal-Cardoso JH, Zin WA and Faffe DS: *In vivo* anti-inflammatory action of eugenol on lipopolysaccharide-induced lung injury. J Appl Physiol *108*: 845-851, 2010.
29 Bachiega TF, de Sousa JP, Bastos JK and Sforcin JM: Clove and eugenol in noncytotoxic concentrations exert immunomodulatory/anti-inflammatory action on cytokine production by murine macrophages. J Pharm Pharmacol *64*: 610-616, 2012.
30 Fujisawa S, Atsumi T, Satoh K, Kadoma Y, Ishihara M, Okada N, Kashiwagi Y, Yokoe I and Sakagami H: Radical generation, radical-scavenging activity and cytotoxicity of eugenol-related compounds. In Vitro Mol Toxicol *13*: 269-279, 2000.
31 Fujisawa S, Atsumi T, Kadoma Y and Sakagami H: Antioxidant and prooxidant action of eugenol-related compounds and their cytotoxicity. Forum "Phenolic compounds: Free radical mechanisms of toxicity, catalysis, and protection". Toxicology *177*: 39-54, 2002.
32 Chang YC, Tai KW, Huang FM and Huang MF: Cytotoxic and nongenotoxic effects of phenolic compounds in human pulp cell cultures. J Endod *26*: 440-443, 2000.
33 Tanaka S, Machino M, Akita S, Yokote Y and Sakagami H: Changes in salivary amino acid composition during aging. In Vivo *24*: 853-856, 2010.
34 Tanaka S, Maehara K, Kaneshima A, Machino M, Onuma H, Kaneko M, Sakagami H, Sugimoto M, Soga T and Tomita M: Pilot study of changes in salivary metabolic profiles induced by template therapy. In Vivo *26*: 1015-1020, 2012.

Received January 8, 2013
Revised January 29, 2013
Accepted January 30, 2013